

**COMPUTATIONAL FLUID DYNAMICS (CFD) SIMULATION OF LOW  
REYNOLDS NUMBER FLOW OVER AIRFOILS FOR UNMANNED AERIAL  
VEHICLE (UAV)**

**by**

**CHAN QUAN XIN**

**Thesis submitted in fulfilment of the requirements for the Bachelor Degree of  
Engineering (Honours) (Aerospace Engineering)**

**June 2019**

## ENDORSEMENT

I, Chan Quan Xin hereby declare that all corrections and comments made by the supervisor and examiner have been taken consideration and rectified accordingly.

---

(Signature of Student)

Date:

---

(Signature of Supervisor)

Name: Assoc. Prof. Dr. Farzad Ismail

Date:

---

(Signature of Examiner)

Name: Dr. Ahmad Zulfaa Mohamed Kassim

Date:

## DECLARATION

This thesis is the result of my own investigation, except where otherwise stated and has not previously been accepted in substance for any degree and is not being concurrently submitted in candidature for any other degree.

---

(Signature of Student)

Date:

## ACKNOWLEDGEMENTS

First and foremost, I would like to express my deepest gratitude to Associate Professor Dr. Farzad Ismail for being my supervisor and advisor. He had provided a lot of assistance and knowledge for me to successfully proceed with my research. It would be a difficult task for me to complete my research without his assistance. Besides, I would like to thank Dr. Ahmad Zulfaa Mohamed Kassim for serving as my examiner to mark this report and also making comment for review of my research. I would also like to thank Dr. Mohammad Hafifi Bin Ishaik for helping me to kick off this research. In addition, I would like to thank Ir. Dr. Nurulasikin Mohd Suhadis for laying out a proper thesis guideline.

Next, I would like to thank the research team that is under supervision of Associate Professor Dr. Farzad Ismail. They are postgraduate student who have a lot of experienced in Computational Fluid Dynamics (CFD). They had given a lot of opinions and guidance during the weekly discussions which provided many ideas for me to proceed my research.

Finally, I would like to thank my friends and family for their emotional support and understanding.

**COMPUTATIONAL FLUID DYNAMICS (CFD) SIMULATION OF LOW  
RENOLDS NUMBER FLOW OVER AIRFOILS FOR UNMANNED AERIAL  
VEHICLE (UAV)**

**ABSTRACT**

The technology of Unmanned Aerial Vehicle (UAV) or commonly known as drone technology is growing fast and rapidly advancing in Malaysia. The growth in this technology is due to an increase of UAV uses for many tasks. In the military field, the UAV is usually used to carry out surveillance mission or even as a combat fighter. Apart from military applications, the UAV is widely involved for research like sending UAV to a hard-to-reach terrain to collect data that is difficult to obtain. Hence, it leads to a growing interest in research of UAV to build a better UAV. A good UAV is normally accompanied with some of the features such as equipped with high payload, shortened take-off and landing distances, lower stall speed and a high lift airfoil with low Re number. Thus, the project focuses on the high lift airfoil with low Re to have a lower stall speed as well as a large enough of lift produced. Two cambered airfoils will be chosen for aerodynamic analysis with Re number lower than 100,000. The limitation of Re number is to ensure the air flow over the airfoils are fully laminar. The analysis is conducted using computational fluid dynamics simulation software which is Fluent. A 2D geometry is first plot using Design Modeler. Meshing is generated for each airfoil after import from Design Modeler. The meshing is then read into Fluent to perform simulation and the result such as graph of lift coefficient at different AOA and graph of drag coefficient at different AOA are used to compare the aerodynamic characteristics of each airfoil.

**SIMULASI BERKOMPUTER DINAMIK BENDALIR DENGAN ALIRAN  
NOMBOR REYNOLDS YANG RENDAH BAGI AIRFOIL UNTUK PESAWAT  
UDARA TANPA PEMANDU**

**ABSTRAK**

Teknologi pesawat udara tanpa pemandu (UAV) atau yang dikenali sebagai teknologi drone berkembang pesat di Malaysia. Pertumbuhan dalam teknologi ini disebabkan peningkatan penggunaan UAV untuk banyak tugas. Dalam bidang ketenteraan, UAV biasanya digunakan untuk menjalankan misi pengawasan atau bahkan sebagai pejuang tempur. Selain daripada aplikasi ketenteraan, UAV terlibat secara meluas untuk penyelidikan seperti menghantar UAV ke medan yang sukar dicapai untuk mengumpulkan data yang sukar diperolehi. Oleh itu, ia membawa kepada minat yang semakin meningkat dalam penyelidikan UAV untuk membina UAV yang lebih baik. UAV yang baik biasanya disertakan dengan beberapa ciri seperti dilengkapi dengan muatan yang tinggi, memendekkan jarak jauh dan pendaratan, kelajuan gerai yang lebih rendah dan airfoil berdaya angkat tinggi dengan nombor Re yang rendah. Oleh itu, projek ini memfokuskan pada airfoil berdaya angkat tinggi dengan Re yang rendah untuk mempunyai kelajuan gerai yang lebih rendah dan juga daya angkat yang cukup besar yang dihasilkan. Dua airfoil cambered akan dipilih untuk analisis aerodinamik dengan nombor Re lebih rendah daripada 100,000. Keterbatasan nombor Re adalah untuk memastikan aliran udara ke atas lelayang udara adalah laminar sepenuhnya. Analisis ini dilakukan menggunakan perisian simulasi berkomputer dinamik bendalir seperti Fluent. Geometri 2D adalah plot pertama menggunakan Design Modeler. Meshing dihasilkan untuk setiap airfoil selepas import dari Design Modeler. Meshing kemudian dibaca kepada Fluent

untuk melakukan simulasi dan hasilnya seperti graf pekali daya angkat terhadap AOA yang berbeza dan graf pekali daya seret terhadap AOA yang berbeza digunakan untuk membandingkan ciri aerodinamik setiap airfoil.

## TABLE OF CONTENTS

<b>ENDORSEMENT</b>	i
<b>DECLARATION</b>	ii
<b>ACKNOWLEDGEMENTS</b>	iii
<b>ABSTRACT</b>	iv
<b>ABSTRAK</b>	v
<b>LIST OF FIGURES</b>	ix
<b>LIST OF ABBREVIATIONS</b>	xiii
<b>LIST OF SYMBOLS</b>	xiv
<b>CHAPTER</b>	
<b>1 INTRODUCTION</b>	1
1.1 Problem Statement	1
1.2 Objectives	1
1.3 Background of Airfoils	1
1.4 Background of Unmanned Aerial Vehicle (UAV)	2
<b>2 LITERATURE REVIEW</b>	4
2.1 Airfoil Comparison	4
<b>3 METHODOLOGY</b>	7
3.1 Methods and Techniques	7
3.1.1 Designing of Airfoils	7
3.1.2 Meshing of Domain	12
3.1.3 Setup of Simulation	15
3.2 Result Validation	23
<b>4 RESULT AND DISCUSSION</b>	25
4.1 Validation of Results	25
4.1.1 Number of Meshing	25
4.1.2 Different Order of Accuracy Upwind Scheme	28
4.1.3 Result Comparison with Experimental Value	32
4.2 Airfoil Simulation Results	36
4.2.1 Simulation Result for E387	37
4.2.2 Simulation Result for NACA 2408	44
4.2.3 Comparison between E387 and NACA 2408	53
<b>5 CONCLUSION AND RECOMMENDATIONS</b>	57
5.1 Conclusion	57
5.2 Recommendations	58
5.2.1 Improvements of Solution	58
5.2.2 Future Work	59
<b>REFERENCES</b>	60
<b>APPENDICES</b>	62



A - Tabulation of lift coefficient, drag coefficient and lift-to-drag ratio for E387 and NACA 2408	62
B - Tabulation of lift coefficient and drag coefficient for simulation and experimental value using E387 at $Re = 61500$ with compared AOA	63
C- Pressure contour for E387 from AOA of $-4^\circ$ to $16^\circ$	64
D- Pressure contour for NACA 2408 from AOA of $-4^\circ$ to $16^\circ$	70

## LIST OF FIGURES

Figure 2. 1: Comparison between symmetrical airfoils, $Re = 10^4$ (Sauvageat, 2016)	5
Figure 2. 2: Comparison between symmetrical airfoils, $Re = 2 \times 10^4$ (Sauvageat, 2016)	5
Figure 2. 3: Graph of lift coefficient against AOA for NACA 0015 and NACA 4415 (Rubel et al., 2016)	6
Figure 3. 1: Extracting airfoil point coordinates for airfoil E387 (Tool, 2019)	8
Figure 3. 2: Joining all the guiding points using curve line feature (Design Modeler)	9
Figure 3. 3: Creating the airfoil surface body (Design Modeler)	9
Figure 3. 4: Creating a domain surrounding the airfoil (Design Modeler)	10
Figure 3. 5: Separating the domain into four parts (Design Modeler)	10
Figure 3. 6: Creating surface body for the domain (Design Modeler)	11
Figure 3. 7: The airfoil surface body (center hollow part) is cut out from the domain surface body (Design Modeler)	12
Figure 3. 8: Edge sizing is created for each edge (ANSYS Meshing)	13
Figure 3. 9: Face meshing is created for mapping the 4 faces (ANSYS Meshing)	13
Figure 3. 10: Meshing of the domain is created (ANSYS Meshing)	14
Figure 3. 11: Magnified of meshing around the airfoil (ANSYS Meshing)	14
Figure 3. 12: Element quality and number of nodes & elements (ANSYS Meshing)	15
Figure 3. 13: General setting in Fluent (ANSYS Fluent)	16
Figure 3. 14: Selection of viscous model in Fluent (ANSYS Fluent)	17
Figure 3. 15: Selection of materials in Fluent (ANSYS Fluent)	18
Figure 3. 16: Setting for boundary conditions (ANSYS Fluent)	18

Figure 3. 17: Defining boundary conditions (ANSYS Fluent)	19
Figure 3. 18: Velocity inlet for inlet boundary condition (ANSYS Fluent)	19
Figure 3. 19: Wall boundary condition for airfoil body (ANSYS Fluent)	20
Figure 3. 20: Setting for solution methods in Fluent (ANSYS Fluent)	21
Figure 3. 21: Solution controls by under-relaxation factors (ANSYS Fluent)	22
Figure 3. 22: Number of iterations for running calculation (ANSYS Fluent)	23
Figure 3. 23: Summary of Low-Speed Airfoil Data by Michael S.Selig (Selig et al., 1995)	24
Figure 4. 1: Lift coefficient against number of meshing for AOA of $0.92^\circ$ using second order upwind scheme	26
Figure 4. 2: Drag coefficient against number of meshing for AOA of $0.92^\circ$ using second order upwind scheme	27
Figure 4. 3: Lift coefficient against number of meshing for AOA of $0.92^\circ$ using first order upwind scheme	29
Figure 4. 4: Drag coefficient against number of meshing for AOA of $0.92^\circ$ using first order upwind scheme	29
Figure 4. 5: Velocity contour for first order upwind scheme for AOA of $0.92^\circ$	30
Figure 4. 6: Velocity contour for second order upwind scheme for AOA of $0.92^\circ$	31
Figure 4. 7: Velocity vector at trailing edge for second order upwind scheme for AOA of $0.92^\circ$	32
Figure 4. 8: Lift coefficient against AOA for simulation and experimental value	33
Figure 4. 9: Velocity contour for AOA of $-5.36^\circ$	34
Figure 4. 10: Velocity vector for AOA of $-5.36^\circ$	35

Figure 4. 11: Drag coefficient against AOA for simulation and experimental value	36
Figure 4. 12: Lift coefficient against AOA for E387	37
Figure 4. 13: Drag coefficient against AOA for E387	38
Figure 4. 14: Velocity contour for E387 at AOA of $-4^\circ$	39
Figure 4. 15: Velocity contour for E387 at AOA of $-2^\circ$	39
Figure 4. 16: Velocity contour for E387 at AOA of $0^\circ$	40
Figure 4. 17: Velocity contour for E387 at AOA of $2^\circ$	40
Figure 4. 18: Velocity contour for E387 at AOA of $4^\circ$	41
Figure 4. 19: Velocity contour for E387 at AOA of $6^\circ$	41
Figure 4. 20: Velocity contour for E387 at AOA of $8^\circ$	42
Figure 4. 21: Velocity contour for E387 at AOA of $10^\circ$	42
Figure 4. 22: Velocity contour for E387 at AOA of $12^\circ$	43
Figure 4. 23: Velocity contour for E387 at AOA of $14^\circ$	43
Figure 4. 24: Velocity contour for E387 at AOA of $16^\circ$	44
Figure 4. 25: Lift coefficient against AOA for NACA 2408	45
Figure 4. 26: Drag coefficient against AOA for NACA 2408	46
Figure 4. 27: Velocity contour for NACA 2408 at AOA of $-4^\circ$	47
Figure 4. 28: Velocity contour for NACA 2408 at AOA of $-2^\circ$	47
Figure 4. 29: Velocity contour for NACA 2408 at AOA of $0^\circ$	48
Figure 4. 30: Velocity contour for NACA 2408 at AOA of $2^\circ$	48
Figure 4. 31: Velocity contour for NACA 2408 at AOA of $4^\circ$	49
Figure 4. 32: Velocity contour for NACA 2408 at AOA of $6^\circ$	49
Figure 4. 33: Velocity contour for NACA 2408 at AOA of $8^\circ$	50

Figure 4. 34: Velocity contour for NACA 2408 at AOA of 10°	50
Figure 4. 35: Velocity contour for NACA 2408 at AOA of 12°	51
Figure 4. 36: Velocity contour for NACA 2408 at AOA of 14°	51
Figure 4. 37: Velocity contour for NACA 2408 at AOA of 16°	52
Figure 4. 38: Lift coefficient against AOA for both airfoils	53
Figure 4. 39: Details for both E387 and NACA 2408 ((Tool, 2019))	54
Figure 4. 40: Drag coefficient against AOA for both airfoils	55
Figure 4. 41: Lift-to-drag ratio against AOA for both airfoils	55

## LIST OF ABBREVIATIONS

2D	: Two-dimensional
3D	: Three-dimensional
AOA	: Angle of attack
CFD	: Computational Fluid Dynamics
HPC	: High-performance computing
UAV	: Unmanned aerial vehicle

## LIST OF SYMBOLS

$\alpha$	: Angle of attack
$C_l$	: Lift coefficient
$C_d$	: Drag coefficient
Re	: Reynolds number based on chord length
$\rho$	: Density
$\mu$	: Viscosity
c	: Chord length
V	: Velocity
$\rho_a$	: Air density
v	: Air speed
L/D	: Lift-to-drag ratio

## **CHAPTER 1**

### **INTRODUCTION**

This chapter presents a quick review on the problem statement, objective and background of the airfoil and Unmanned Aerial Vehicle (UAV).

#### **1.1 Problem Statement**

The number of uses of UAV for different purposes is increasing nowadays. However, there is still some issues surrounding current UAVs such as the capability of flight altitude. The capability of flying in a higher altitude can be achieved by having a greater lift coefficient produced by the wing. It is also said to be ideal for having a lower stall speed or shortened take-off and landing distances. Lower stall speed allows the UAV to achieve a lower speed without stalling and the shortened take-off and landing distances will allow the UAVs to take-off or landing in a short run way. which leads to an interest of comparing different airfoils and obtain the best aerodynamic characteristic airfoil.

#### **1.2 Objective**

The objective of conducting this research is to compare different airfoils using computational simulation that will be carried out in Fluent and analysis will be made to obtain the best aerodynamic characteristic airfoil.



### **1.3 Background of Airfoil**

Airfoil is a cross-sectional shape that is normally used for a wing, blades of the propeller or rotor and even sail. Airfoil is used to produce aerodynamic force which consists of lift that its direction is perpendicular to the direction of the motion and drag that its direction is parallel to the direction of the motion. Lift can be generated by a symmetrical airfoil at positive AOA or by a cambered airfoil even at zero AOA. The lift is generated due to the pressure difference which is accompanied by a velocity difference according to Bernoulli's principle. The upper surface of the airfoil has a lower pressure due to higher velocity while lower surface of the airfoil has a higher pressure with a lower velocity when flow is passing over the airfoil.

Development of airfoil began in the late 1800's. In that time, it was a known fact that even a flat plate can produce lift if it is set at an angle of incidence. However, there were some people who suspected that a shape with curvature that is designed to be similar as a bird wing can generate a higher lift. In 1884, a man named H.F Phillips carried out a test on a series of airfoil shapes using the earliest wind tunnels that the air was produced from induction by a steam jet in a wooden trunk. He was then patented those tested airfoil shapes. (Gupta, 2009)

### **1.4 Background of Unmanned Aerial Vehicle (UAV)**

UAV is an aircraft that is driverless in other word, without a human pilot onboard. It is usually referred as drone. Normally, UAV functions as a component with the help of other components such as a ground-based controller and a communication system that

connects each of them. To date, UAV is widely used in military and commercial. For military applications, UAV is usually used as a surveillance tool that scout and collect data from the battlefield or enemy. Apart from that, UAV is well-known for its agricultural usage such as spraying the insecticides as it can save a lot of human work labor and time. Sometimes, UAV is used to collect data from hard-to-reach terrain such as volcano for research purpose.

For the history of UAV, the earliest application of UAV is in 1849 when the Austrians attacked Venice, the Italian city using unmanned balloon that were loaded with explosives. This technology was further developed when the British military used aerial photography during the Battle of Neuve Chapelle in 1915. After that, UAV technology was kept on developing and used for many other military purposes by a few countries such as United State and Israel. Until 2014, this technology has been switched from military application to commercial use when Amazon proposed using UAVs to deliver packages to customers.(O'Donnell, 2017)

## **CHAPTER 2**

### **LITERATURE REVIEW**

This chapter presents a critical review of literature related to the comparison of different airfoils. Several researches that is related will be reviewed and analyzed.

#### **2.1 Airfoils Comparison**

In term of thickness of the airfoil, thinner airfoils are found that generally have higher lift at range of low Re (10,000 – 100,000) in Eric Sauvageat's MES semester project report.(Sauvageat, 2016) In this report, we can tell that thinner airfoils will produce higher lift and smaller drag at low AOA at range of low Re. However, the drag is seeming to be increasing faster at higher AOA for thinner airfoils compared to thicker airfoils. In the report, this fact is shown by comparing a few of symmetrical airfoils with different thickness ranging from the thinnest airfoil NACA0005 to the thickest airfoil NACA0021.

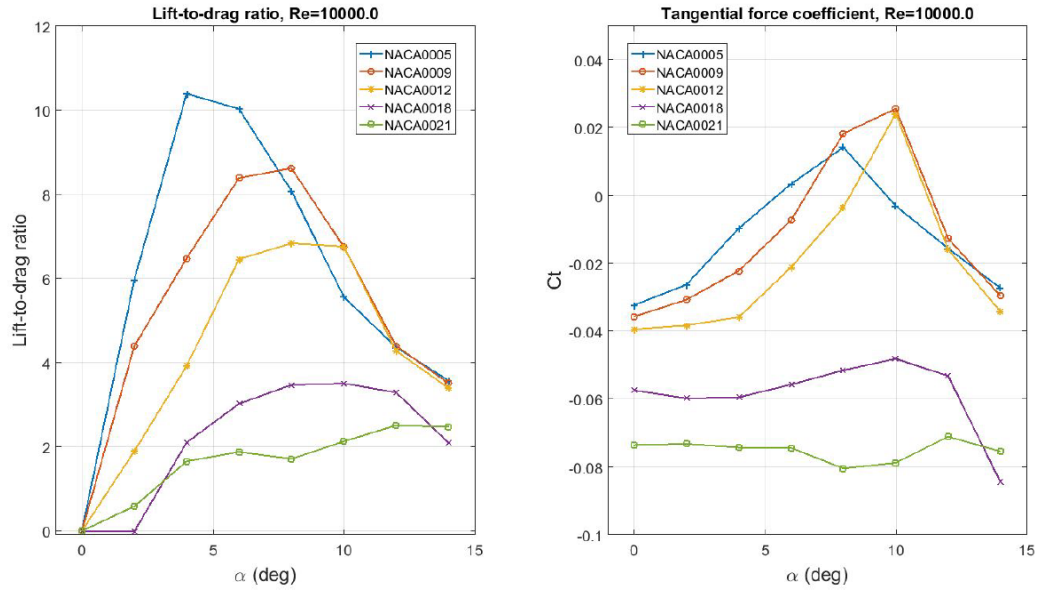


Figure 2. 1: Comparison between symmetrical airfoils,  $Re = 10^4$  (Sauvageat, 2016)

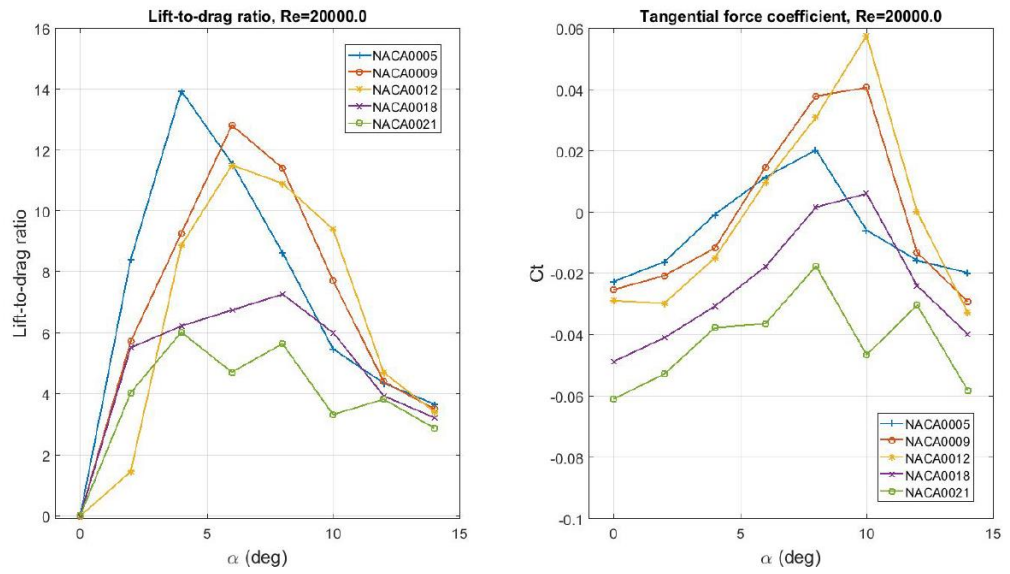


Figure 2. 2: Comparison between symmetrical airfoils,  $Re = 2 \times 10^4$  (Sauvageat, 2016)

For the shape of airfoil, cambered airfoil is found to be generating a higher lift coefficient than a symmetrical airfoil which can be found in a review of “Comparison of Aerodynamics Characteristics of NACA 0015 & NACA 4415” (Rubel et al., 2016). From this review, it is analyzed that there is a larger negative pressure created on the cambered airfoil (NACA 4415) than a symmetrical airfoil (NACA 0015) which leads to a larger lift generated.

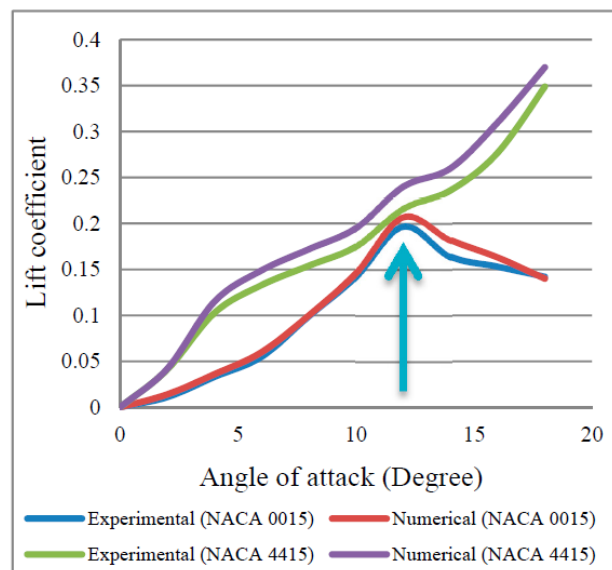


Figure 2. 3: Graph of lift coefficient against AOA for NACA 0015 and NACA 4415 (Rubel et al., 2016)

## **CHAPTER 3**

### **METHODOLOGY**

This chapter presents the methods and techniques used, experiment design and validation method for this research.

#### **3.1 Methods and Techniques**

Computational simulation on airfoil is performed for this research. Unlike physical experiment, the model which is the airfoil will need to be drawn and the drawing will be used in the simulation software. Aerodynamic characteristic of the airfoil will be tested and analyzed after the simulation is done.

##### **3.1.1 Designing of Airfoil**

A designing software is needed to draw the airfoil. In this research, Design Modeler is used to draw the airfoil and the domain around the airfoil as well. Design Modeler is a software that is readily to be used in ANSYS. (ANSYS, 2019d) ANSYS is a software that capable to carry out physics simulation such as fluid dynamics, heat transfer, vibration, etc. (ANSYS, 2019c)

It is difficult to draw an airfoil without any guiding points. Thus, the required airfoil point coordinates can be extracted from a website named “Airfoil Tools”. (Tool, 2019)

The screenshot shows the 'Airfoil Tools' website interface. At the top, there is a search bar with '1636 airfoils' and a 'Google Custom Search' button. Below the search bar, the main content area displays 'E387 (e387-il)' and 'E387 - Eppler E387 low Reynolds number airfoil'. A large red airfoil profile is shown on a grid. Below the profile, there are three sections: 'Details', 'Dat file', and 'Parser'. The 'Dat file' section shows a table of coordinates for the airfoil.

Dat file	
E387	
1.00000	0.00000
0.99677	0.00043
0.98729	0.00180
0.97198	0.00423
0.95128	0.00763

Figure 3. 1: Extracting airfoil point coordinates for airfoil E387 (Tool, 2019)

The extracted airfoil point coordinates are saved in a text file and it is then read into Design Modeler to create guiding points.

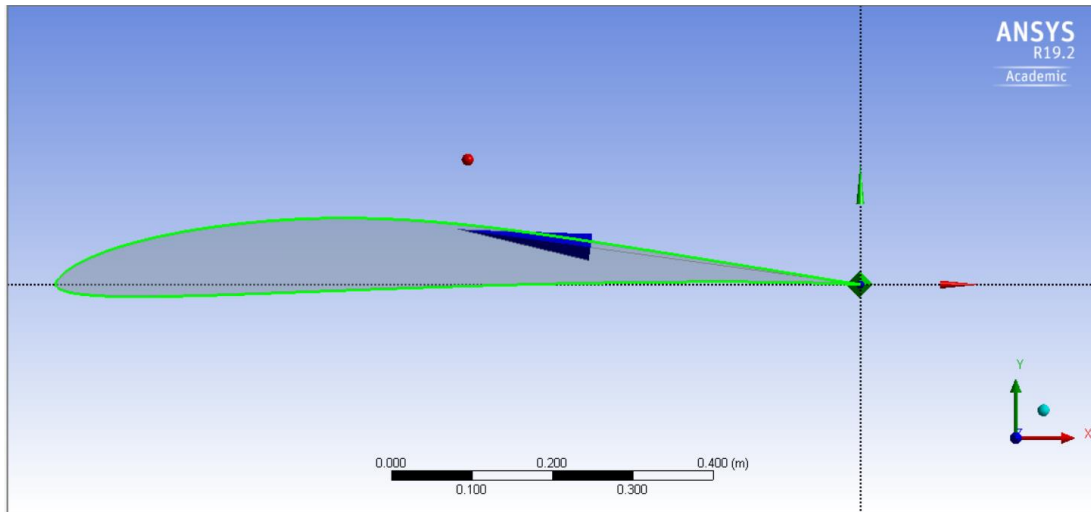


Figure 3. 2: Joining all the guiding points using curve line feature (Design Modeler)

As shown in Figure 3.2, the green line indicated the curve line joined between the guiding points.

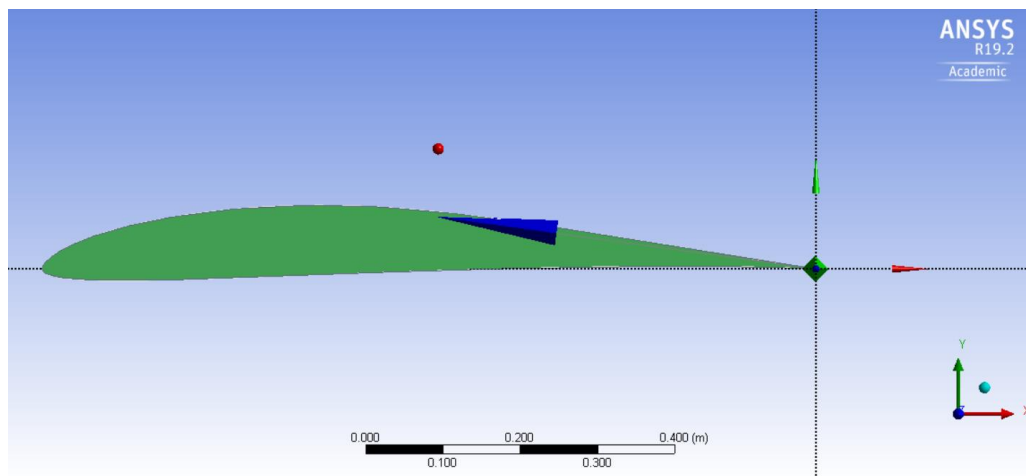


Figure 3. 3: Creating the airfoil surface body (Design Modeler)

After having all the guiding points joined by using the curve line, the entire enclosed area is used to form a surface body.



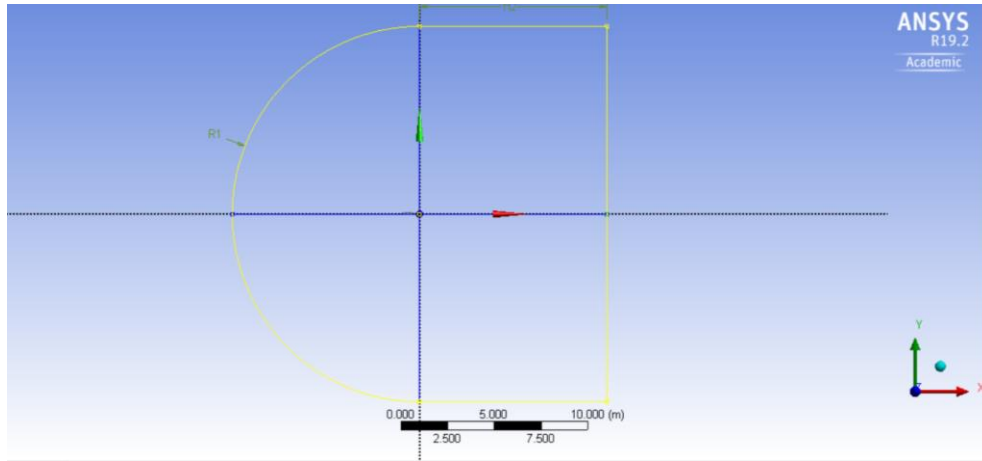


Figure 3. 4: Creating a domain surrounding the airfoil (Design Modeler)

A domain that is surrounding the airfoil is needed for carry out the flow simulation around the airfoil. In Figure 3.4, the highlighted yellow line indicates the domain which is designed in a C-shape. The front part which is curvature part is designed as 10m as its radius value and the part behind is designed as 10m for both length and height.

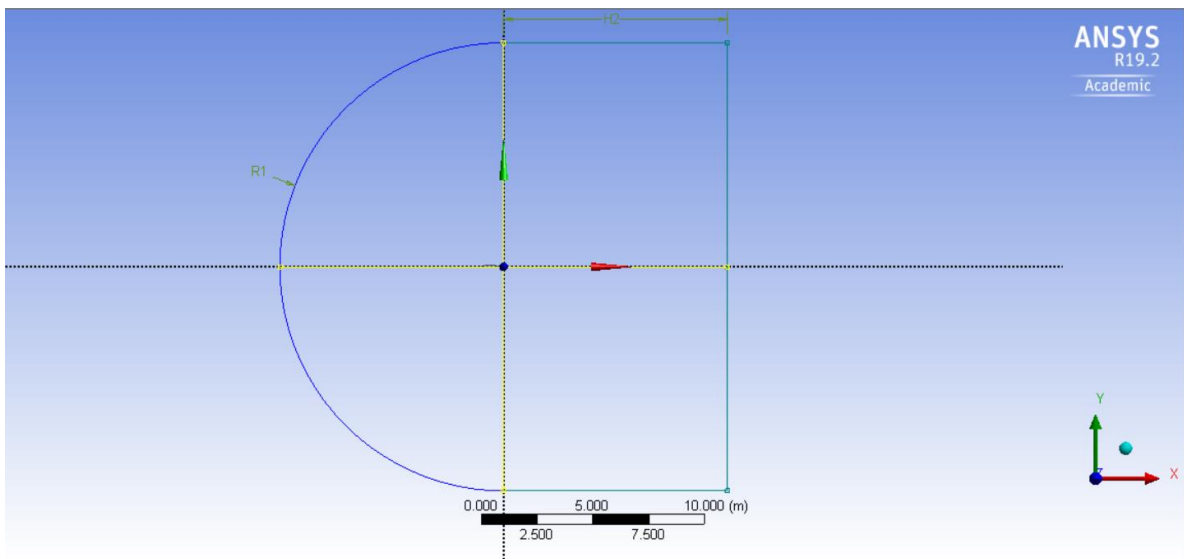


Figure 3. 5: Separating the domain into four parts (Design Modeler)

Two straight lines which is indicated as the yellow lines in Figure 3.5 is drawn to separate the domain into four parts. This is done to make sure a finer meshing at the center around the airfoil can be produced during the later meshing.

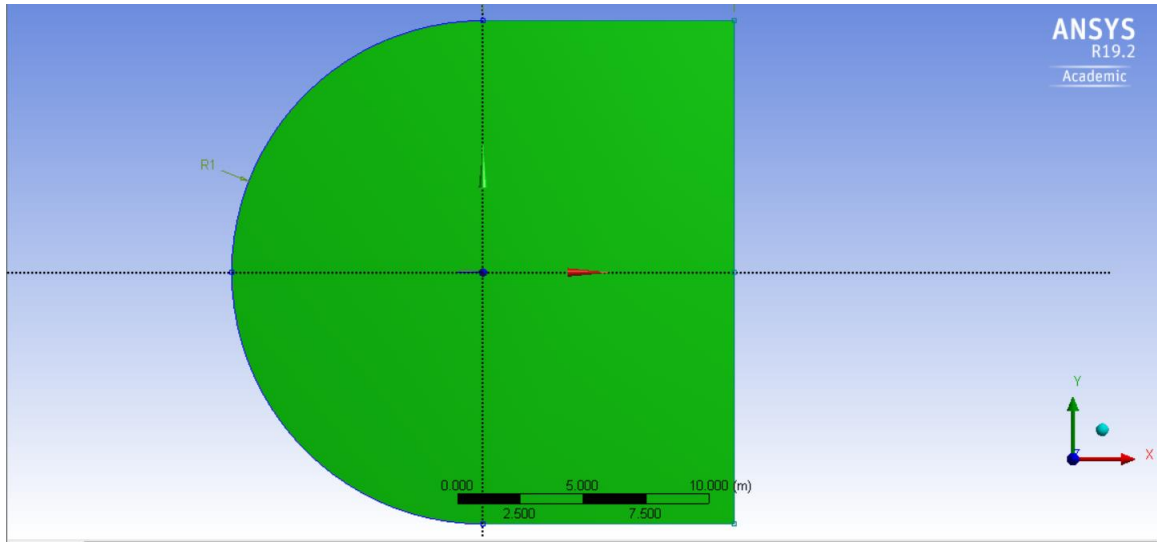


Figure 3. 6: Creating surface body for the domain (Design Modeler)

The enclosure area of the domain is then formed as a surface body. However, the surface body of the airfoil is included inside the surface body of the domain as well. Thus, the surface body of the airfoil is then cut out from the domain surface body using Boolean feature.

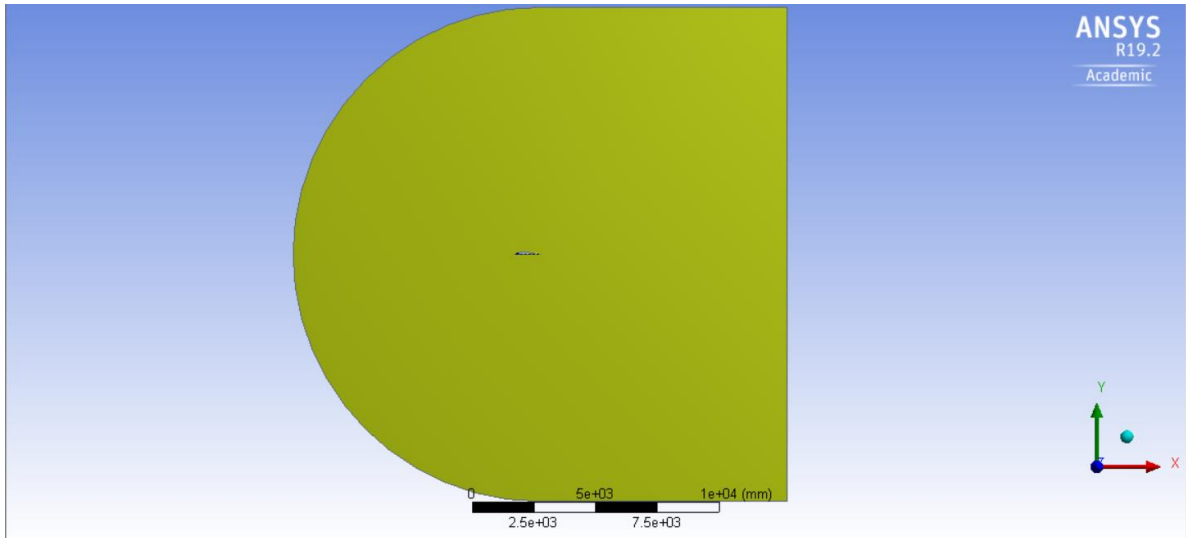


Figure 3. 7: The airfoil surface body (center hollow part) is cut out from the domain surface body (Design Modeler)

### 3.1.2 Meshing of Domain

After the drawing is done in Design Modeler, it is read into another software which is ANSYS Meshing. ANSYS Meshing is a general-purpose, intelligent and automated high-performance product that is built inside ANSYS. It is used to create mesh for solving any physics problems. (ANSYS, 2019b)

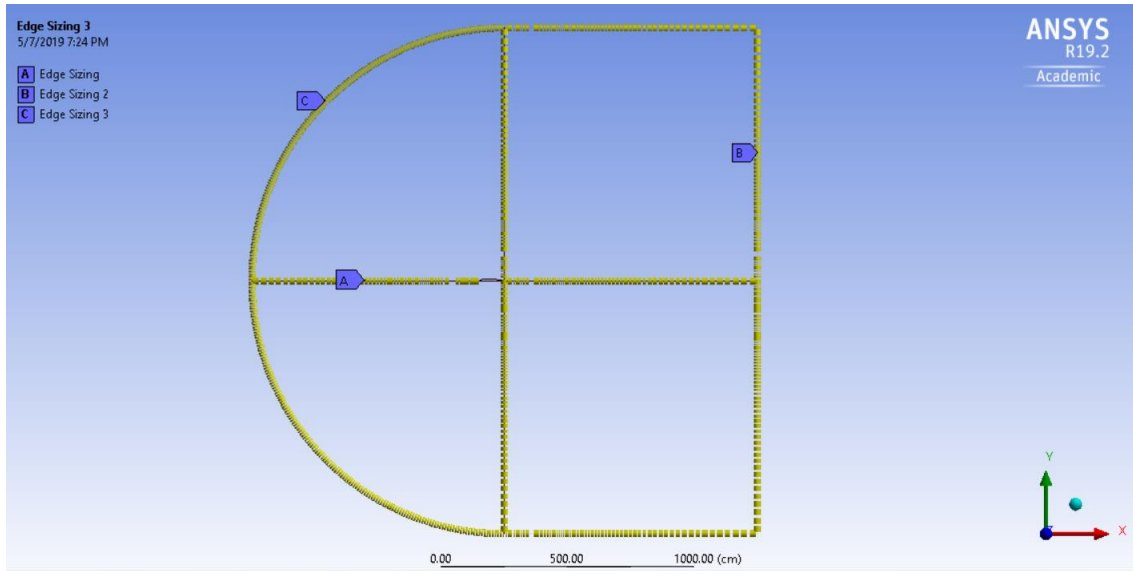


Figure 3. 8: Edge sizing is created for each edge (ANSYS Meshing)

Edge sizing is used to create the mesh. Type of edge size is number of divisions with 150 divisions.

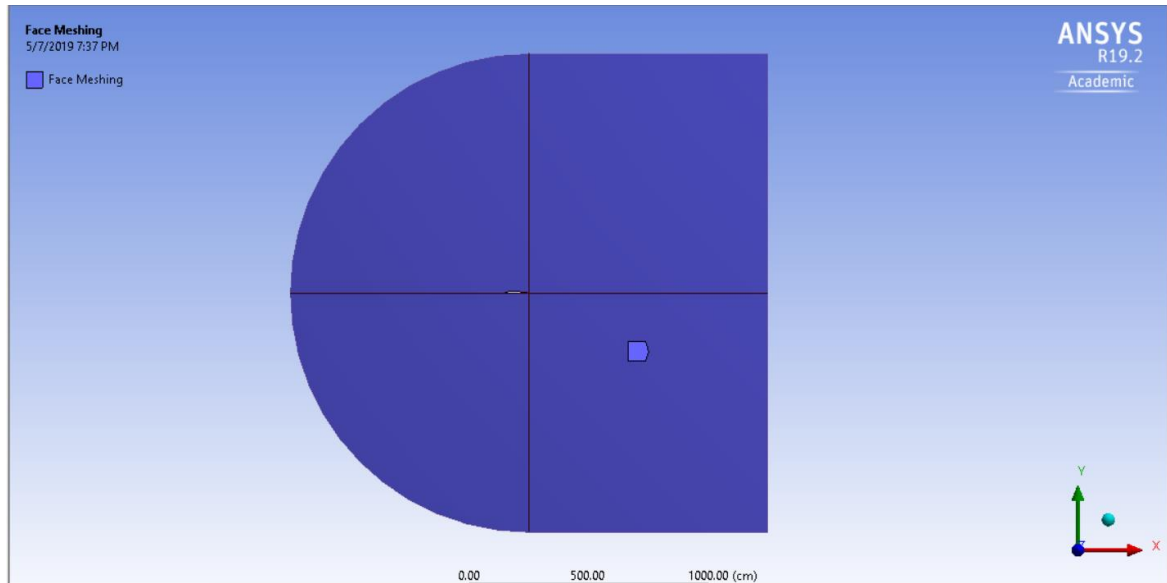


Figure 3. 9: Face meshing is created for mapping the 4 faces (ANSYS Meshing)

After edge sizing is created, face meshing is used for mapping the 4 faces.

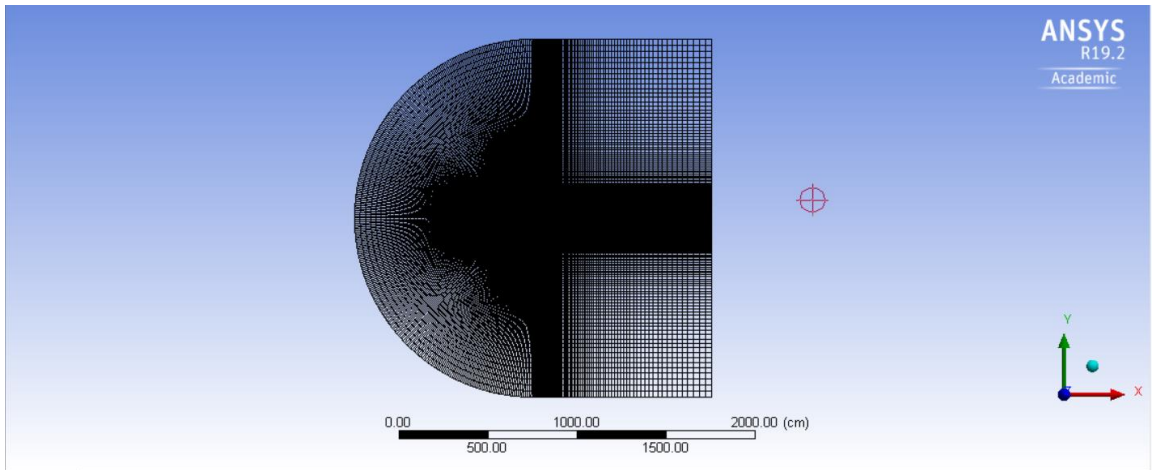


Figure 3. 10: Meshing of the domain is created (ANSYS Meshing)

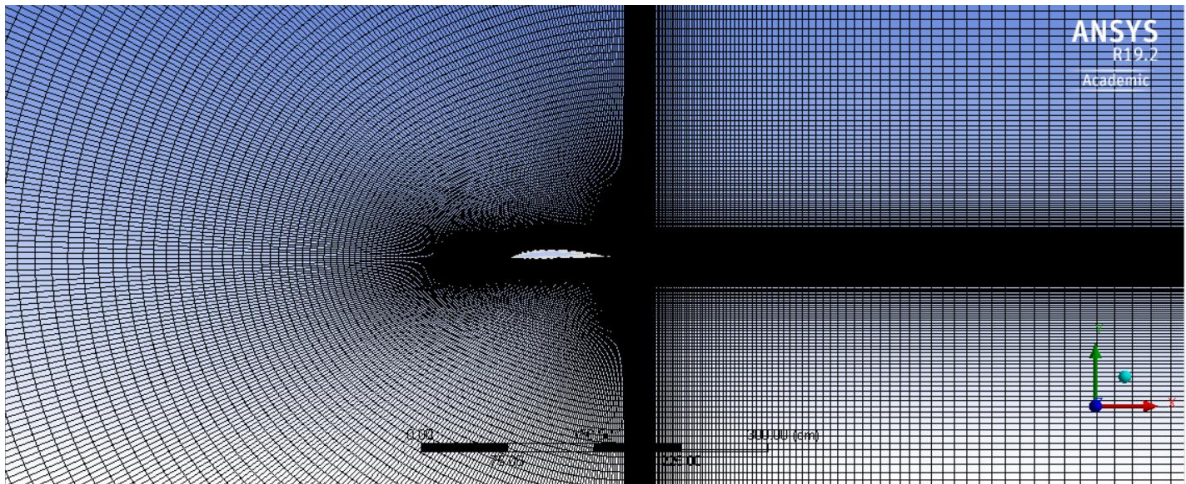


Figure 3. 11: Magnified of meshing around the airfoil (ANSYS Meshing)

The meshing is done after creating edge sizing and face meshing. Figure 3.10 shows the final meshing of the domain while Figure 3.11 shows the magnified part of the meshing which is the center and the meshing around the airfoil.

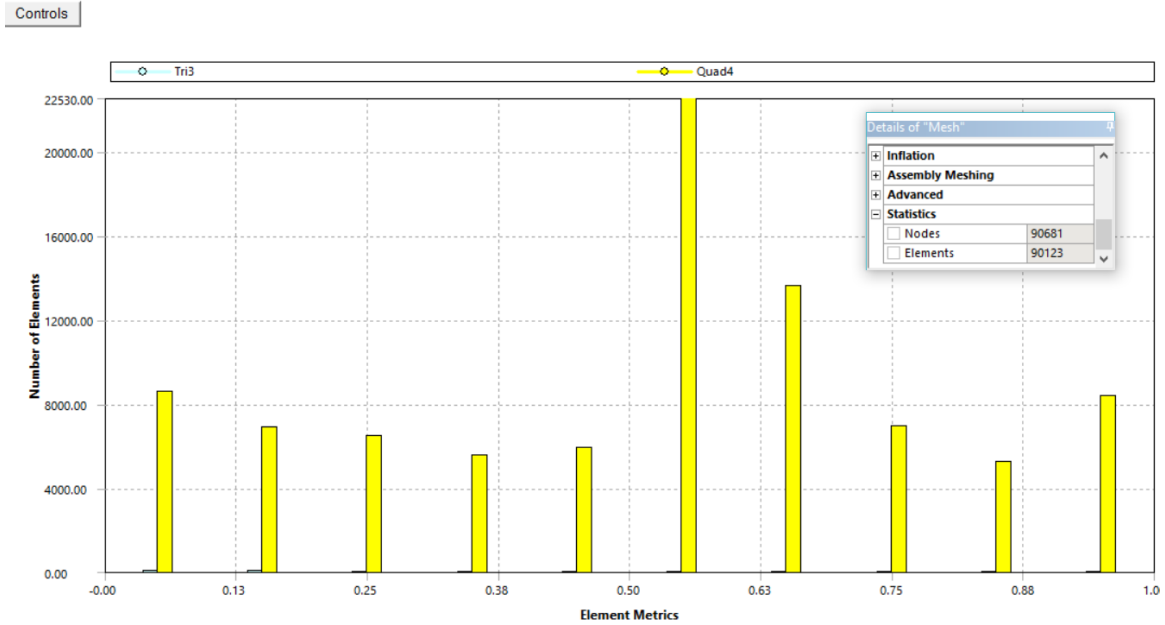


Figure 3. 12: Element quality and number of nodes & elements (ANSYS Meshing)

Figure 3.12 shows the element quality of the meshing. Most of the mesh is beyond 0.5 which indicates an acceptable quality for the meshing. The total number of nodes for the meshing is 90681 while the number of elements is 90123.

### 3.1.3 Setup of Simulation

Simulation is ready to be carried out after the meshing part is done. Before that, the simulation is carried out in Fluent and a preparation setting up of simulation is needed. Fluent is a software that is used to model flow, turbulence, heat transfer and reactions for industrial applications. Fluent provides highly scalable and high-performance computing (HPC) for solving large and complex model computational fluid dynamics (CFD) simulations quickly and cost-effectively. (ANSYS, 2019a)

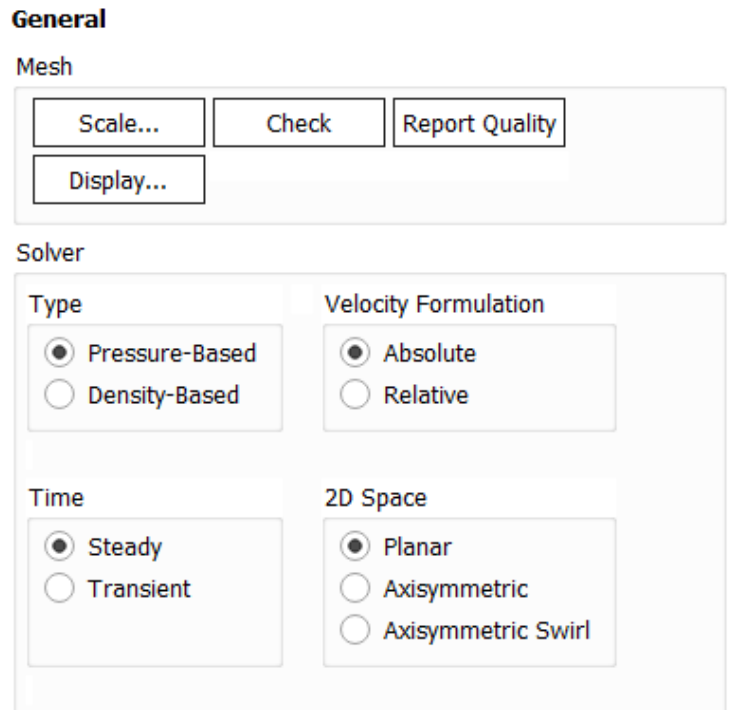


Figure 3. 13: General setting in Fluent (ANSYS Fluent)

Under the solver tab, Pressure-Based is selected for type of solver. The difference between Pressure-Based and Density-Based is that Pressure-Based is used to solve low-speed incompressible flow while Density-Based is used to solve high speed compressible flow. (SAS IP, 2016b) For the next option which is between steady and transient, steady is chosen for selection of time. In this research, the flow throughout the simulation is in steady state which in other word, the fluid properties at any single point of the flow does not change over time. Absolute velocity formulation is selected instead of relative velocity formulation due to most of the flow in this research does not rotates. Planar is selected for the 2D space option as the problem in this research is in 2D.

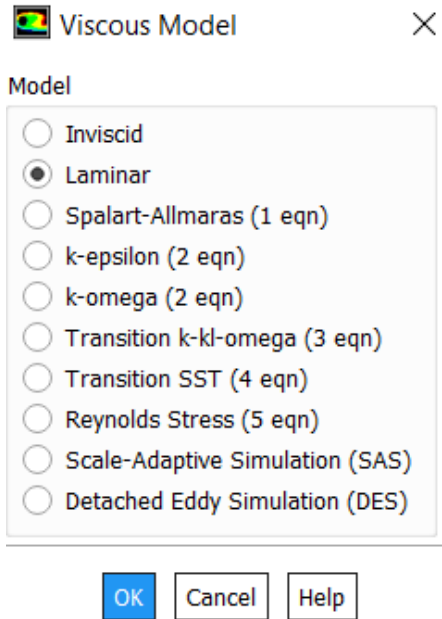


Figure 3. 14: Selection of viscous model in Fluent (ANSYS Fluent)

The first two models which are inviscid and laminar are used for laminar flow. The difference between these two models is that inviscid model does not deal with viscosity while laminar model does deal with viscosity. For the other models, those models are used when dealing with turbulent flow. In this research, viscosity is not neglected, and the flow is laminar, thus, laminar model is chosen.



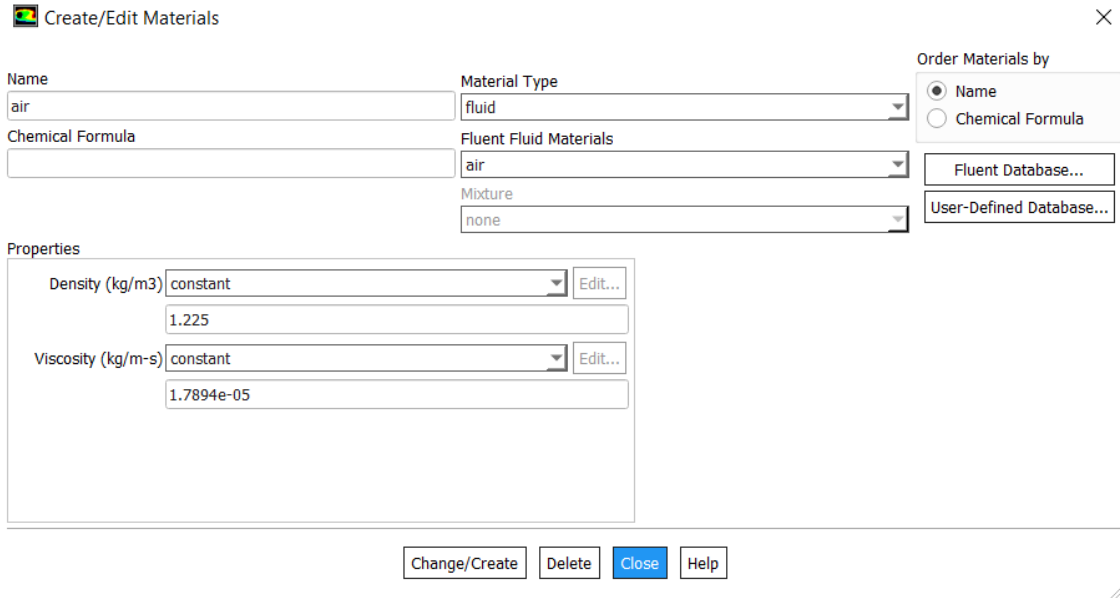


Figure 3. 15: Selection of materials in Fluent (ANSYS Fluent)

Under materials category and under fluid tab, the material is chosen as air with density and viscosity value set to sea-level value.

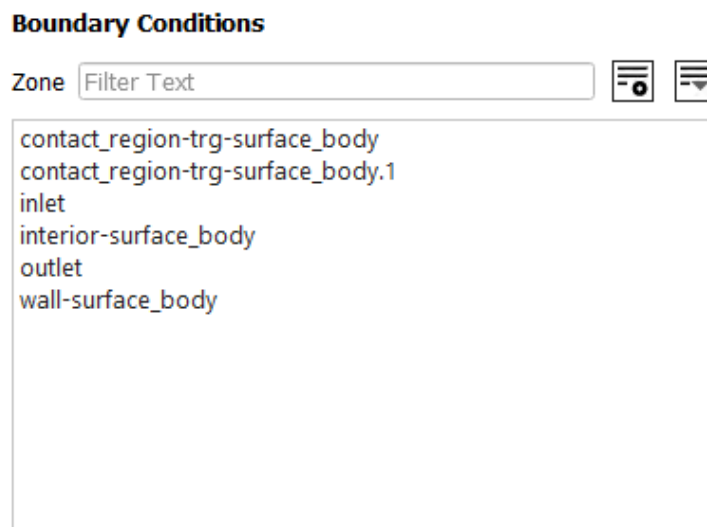


Figure 3. 16: Setting for boundary conditions (ANSYS Fluent)

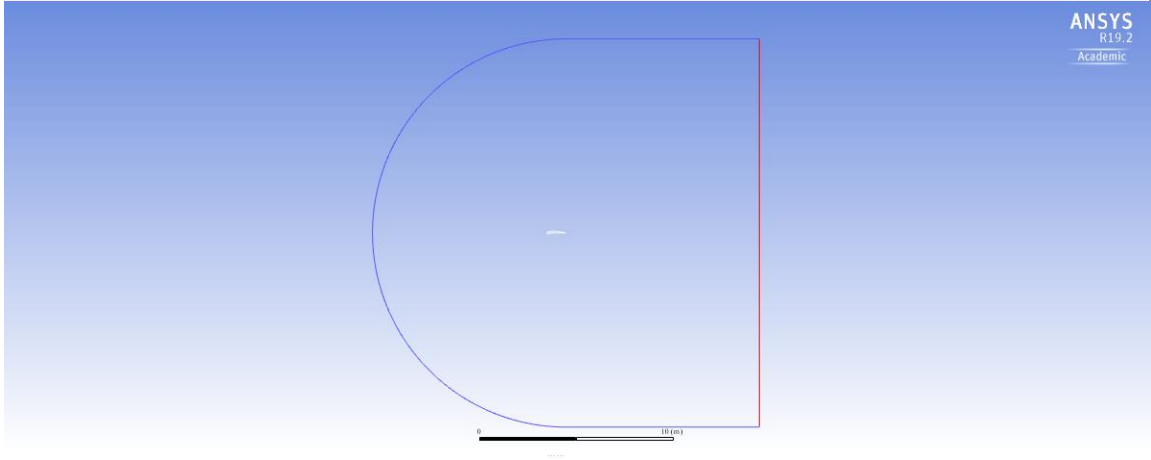


Figure 3. 17: Defining boundary conditions (ANSYS Fluent)

As the image shown in Figure 3.16 and Figure 3.17, the blue line is set as velocity inlet, red line is set as pressure outlet and the middle white section is the airfoil body.

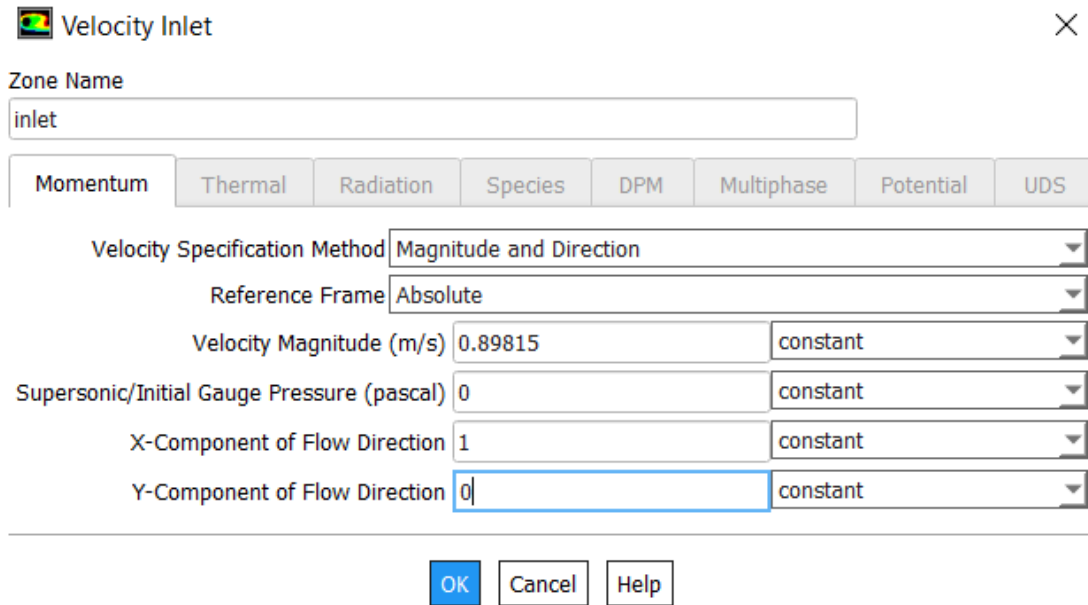


Figure 3. 18: Velocity inlet for inlet boundary condition (ANSYS Fluent)

For velocity inlet, the setting is set as shown in Figure 3.18. The  $Re$  used in this research is 61,500. Using the sea-level value for density and viscosity and chord length equal to 1 m, the velocity can be calculated in equation (3.1),

$$Re = \frac{\rho V c}{\mu} \quad (3.1)$$

In order to set the flow relative to airfoil with an angle of attack, x-component and y-component of flow direction is calculated by taking cosine and sine of the angle.

$$X - component = \cos(\alpha) \quad (3.2)$$

$$Y - component = \sin(\alpha) \quad (3.3)$$

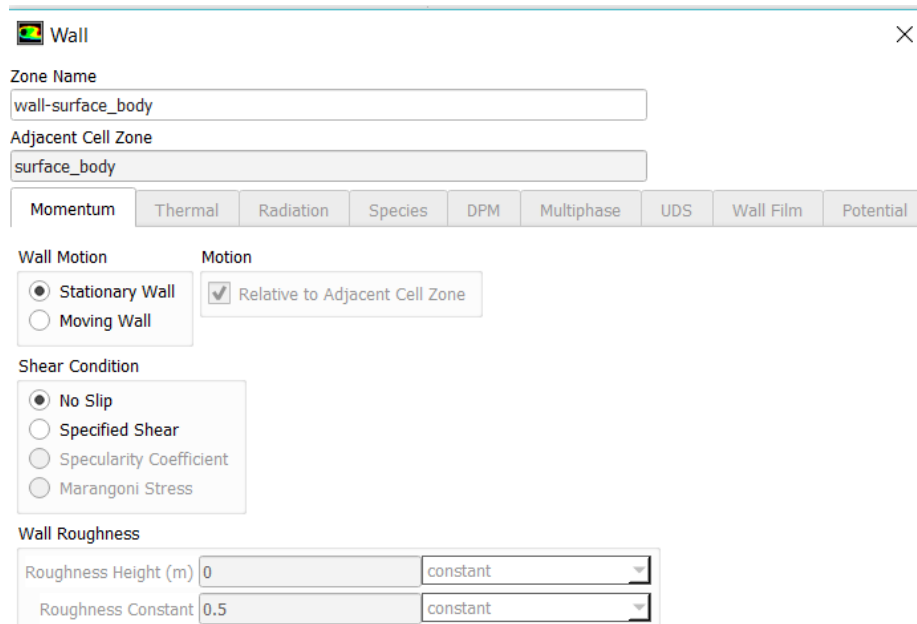


Figure 3. 19: Wall boundary condition for airfoil body (ANSYS Fluent)

For the airfoil body, the wall boundary condition is set as no-slip stationary wall and there will be no shear acting on the airfoil body.

**Solution Methods**

Pressure-Velocity Coupling

Scheme  
SIMPLE

Spatial Discretization

Gradient  
Least Squares Cell Based

Pressure  
Second Order

Momentum  
Second Order Upwind

Transient Formulation

Non-Iterative Time Advancement

Frozen Flux Formulation

Pseudo Transient

Warped-Face Gradient Correction

High Order Term Relaxation

Figure 3. 20: Setting for solution methods in Fluent (ANSYS Fluent)

SIMPLE scheme is used in this research as this scheme is suitable to solve uncomplicated laminar flow problem in which convergence is only limit by pressure-velocity coupling. (SAS IP, 2016a) Second order upwind is used to solve momentum as it is less diffusive and more accurate.

**Solution Controls**

Under-Relaxation Factors

Pressure  
0.2

Density  
1

Body Forces  
1

Momentum  
0.3

Figure 3. 21: Solution controls by under-relaxation factors (ANSYS Fluent)

The value for pressure and momentum is set from default value which is 0.3 and 0.7 to 0.2 and 0.3 respectively to speed up convergence rate.

**Run Calculation**

Check Case...      Update Dynamic Mesh...

Options

Data Sampling for Steady Statistics

Sampling Interval  
1      Sampling Options...

Iterations Sampled 0

Number of Iterations      Reporting Interval  
10000      1

Profile Update Interval  
1

Data File Quantities...      Acoustic Signals...

Figure 3. 22: Number of iterations for running calculation (ANSYS Fluent)

As shown in Figure 3.22, the simulation calculation is hybrid initialized and run with 10000 iterations.

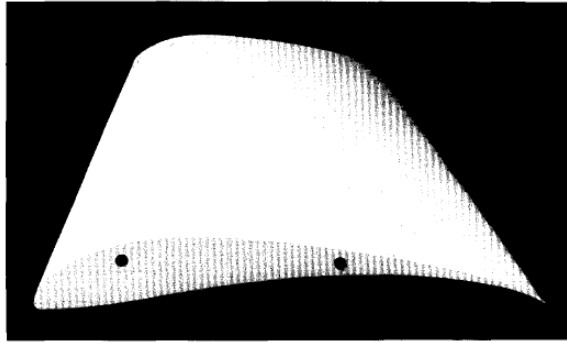
### **3.2 Result Validation**

The result that is obtained through the simulation is not known to be correct or wrong. It is important to validate the simulation result by comparing the result with an experimental result. It can be done by setting up a simulation as similar as possible to the experiment using the same airfoil and same Re that is used in the experiment. In an indirect way, it can increase the trustworthiness of the simulation result.

In this research, the simulation result is compared with experiment result from *Summary of Low Speed Airfoil Data by Michael S.Selig*. (Selig et al., 1995) An airfoil which is E387 will be used in simulation with Re of 61,500. The AOA that will be tested is  $-5.36^\circ$ ,  $0.92^\circ$ ,  $5.4^\circ$  and  $10.13^\circ$ .

## Summary of Low-Speed Airfoil Data

Michael S. Selig, James J. Guglielmo, Andy P. Broeren and Philippe Giguère



Volume 1

Figure 3. 23: Summary of Low-Speed Airfoil Data by Michael S.Selig (Selig et al., 1995)